Int. Journal of Refractory Metals and Hard Materials 41 (2013) 259–269

Contents lists available at ScienceDirect

Int. Journal of Refractory Metals and Hard Materials

journal homepage: www.elsevier.com/locate/IJRMHM

# Experimental investigation on the effect of the material microstructure on tool wear when machining hard titanium alloys: Ti–6Al–4V and Ti-555

M. Nouari *, H. Makich

*University of Lorraine, Laboratoire d'Énergétique et de Mécanique Théorique et Appliquée, LEMTA CNRS-UMR 7563, Mines Nancy, GIP-InSIC, 27 rue d'Hellieule, St-Dié-des-Vosges, France*

ARTICLE INFO

*Article history:*
Received 13 February 2013
Accepted 10 April 2013

*Keywords:*
Machining
β-titanium alloys
Ti-555
Ti–6Al–4V
Tool wear
Microstructure effect

ABSTRACT

An experimental investigation was conducted in this work to analyze the effect of the workpiece microstructure on tool wear behavior and stability of the cutting process during marching difficult to cut titanium alloys: Ti–6Al–4V and Ti-555. The analysis of tool–chip interface parameters such as friction, temperature rise, tool wear and workpiece microstructure evolution under different cutting conditions have been investigated. As the cutting speed increases, mean cutting forces and temperature show different progressions depending on the considered microstructure. Results show that wear modes of cutting tools used for machining the Ti-555 alloy exhibit contrast from those obtained for machining the Ti–6Al–4V alloy. Because of the fine-sized microstructure of the near-β titanium Ti-555, abrasion mode was often found to be the dominate wear mode for cemented cutting tools. However, adhesion and diffusion modes followed by coating delamination process were found as the main wear modes when machining the usual Ti–6Al–4V alloy by the same cutting tools. Moreover, a deformed layer was detected using SEM–EDS analysis from the sub-surface of the chip with β-grains orientation along the chip flow direction. The analysis of the microstructure confirms the intense deformation of the machined surface and shows a texture modification.

© 2013 Elsevier Ltd. All rights reserved.

## 1. Introduction

The past century has witnessed significant advancement in machining hard and difficult to cut materials (refractory materials). Although there have been great advances in the development of cutting tool materials, no equivalent development has been made for cutting titanium alloys due to characteristics of their complex microstructure. Titanium alloys such as Ti–6Al–4V, Ti-555, Ti6242S, and Ti-LCB, are used extensively in the aerospace industry for structural components (compressor blades, disks, castings, and gas turbine engines) due to their superior properties such as excellent strength-to-weight ratio, strong corrosion resistance and ability to retain high strength at high temperatures [1,2]. Recent development projects for Boeing 787 or Airbus A380 planes confirm the increasing use of titanium alloys.

Clément et al. [3,4], have reported that the high-level properties of titanium alloys depend on several strengthening mechanisms such as grain size, solid solution atoms, and precipitation hardening, which all can be tuned during the various forming processing steps, leading to particular microstructures. A deep understanding of the microstructural modifications occurring during manufacturing processes are thus required to allow the improvement of the mechanical performances. Further, the machinability of titanium and its alloys is generally considered to be poor owing to several inherent properties of these materials. Titanium is chemically reactive and, therefore, has a tendency to weld to the cutting tool during machining leading to chipping and premature tool failure [5,6]. In addition, its low thermal conductivity increases the temperature at the tool/workpiece interface, which adversely affects the tool life. Additionally, the high strength maintained at elevated temperature and low modulus of elasticity further impairs the machinability of these materials [6–8].

From a microstructural point of view, elemental titanium presents an allotropic phase transformation at 880 °C between the body-centered cubic (bcc) and hexagonal- close-packed structures stable at high and low temperatures, respectively. The two phases of titanium alloys are known as α phase and β phase respectively [9]. Combinations of working and heat treatment alter the microstructure and change the mechanical properties of the metal. The microstructure and properties can also be affected by adding other elements to titanium. Addition of other elements to pure titanium, i.e. alloying, can alter microstructure and properties as well. Depending on which phase is to be dominant in a particular alloy (α, β or α + β) an alloying element (or group of elements) may be added to pure titanium [3–5]. Thus, one way of classifying alloying elements is according to whether they are α or β stabilizers. Alpha stabilizers are soluble in the α-phase and many act as solid solution strengtheners while also increasing the temperature at which the α-phase is stable. Alpha stabilizers include such elements as Al, Ga, Sn, Ge, and La. Beta stabilizing elements decrease the β transus (i.e., the temperature at which the material transforms to 100% β-phase). As such, these elements increase the range over which the β-phase is stable. Beta-stabilizers may be isomorphous or eutectoid. Isomorphous elements

* Corresponding author at: LEMTA CNRS Laboratory, GIP-InSIC, 27 rue d'Hellieule, 88100 St-Dié, France. Tel.: +33 3 29 42 22 26; fax: +33 3 29 42 18 25.
*E-mail address:* mohammed.nouari@univ-lorraine.fr (M. Nouari).

0263-4368/$ – see front matter © 2013 Elsevier Ltd. All rights reserved.
http://dx.doi.org/10.1016/j.ijrmhm.2013.04.011

**Table 1**
Chemical composition of machined titanium.

| Chemical element | Ti–6Al–4V (wt.%) | Ti-555 (wt.%) |
|---|---|---|
| Al | 5.5 | 5 |
| V | 3.8 | 5 |
| Fe | Max 0.8 | 0.3 |
| Mo | 0 | 5 |
| Cr | 0 | 3 |
| Nb | 0 | 0.5–1.5 |
| Zr | 0 | 0.5–1.5 |

**Table 2**
Mechanical and thermal properties of Ti–6Al–4V and Ti-555.

| | Ti–6Al–4V | Ti-555 |
|---|---|---|
| β transus ($T_\beta$) (°C) | 980 | 856 |
| Density (g/cm$^3$) | 4.43 | 4.65 |
| Tensile elastic modulus (GPa) | 110 | 112 |
| Compressive elastic modulus (GPa) | – | 113 |
| Tensile strength (MPa) | 931 | 1236 |
| Yield strength (MPa) | 862 | 1174 |
| Elongation (%) | 14 | 6 |
| Thermal conductivity at 20 °C (W/m K) | 7.3 | 6.2 |
| Specific heat 20–100 °C (J/kg K) | 709 | 495 |

(such as V, Mo, Nb, Ta, and Re) are soluble in the α-phase while eutectoid elements like (Cr, Fe, Mn, Cu, Ag, Au, Ni, and Co) create a eutectoid phase.

According to Fanning [10], Ti-555 (TIMETAL 555) is a high-strength near-β titanium alloy that was designed for improved productivity and excellent mechanical property combinations, including deep hardenability especially in aeronautical and aerospace industries. According to the same author and to Clément et al. in Refs. [3,4], this recent alloy was designed based on the older Russian alloy VT22 to primarily fulfill high-strength forging applications. A lower-strength state with improved toughness and damage tolerance is under consideration for other parts of aircraft structure [11]. However, being of recent origin, there is a lack of information on machining of this alloy. This is despite the existence of information regarding thermomechanical processing of this family of alloys [12], and the abundance of information available regarding machining of titanium and some of its alloys (notably Ti–6Al–4V) [13]. In the machining field, it is well known that titanium and titanium alloys are hard-to-cut materials. This means that Ti-555 will most likely present engineers with many technical problems to be solved in order to produce net shape components. The effect of the titanium alloy microstructure on tool wear is likely to be one of the leading challenges to be overcome in machining this alloy. As such, the study of the tool wear nature when dealing with this alloy is needed. This paper is dedicated to such a purpose. Here, we introduce the findings of a preliminary study on tests carried out for the Ti-555 and compared with the commonly used alloy Ti–6Al–4V. The aim of this research work is to understand the effect of the workpiece microstructure on the tool wear behavior, and the correlation between mechanical and thermal properties of the work material, tool wear, and cutting parameters.

## 2. Experiments

### 2.1. Workpiece material before and after machining

Experiments (orthogonal cutting tests) were conducted for studying machining characteristics of metallic alloys as cutting forces, chip

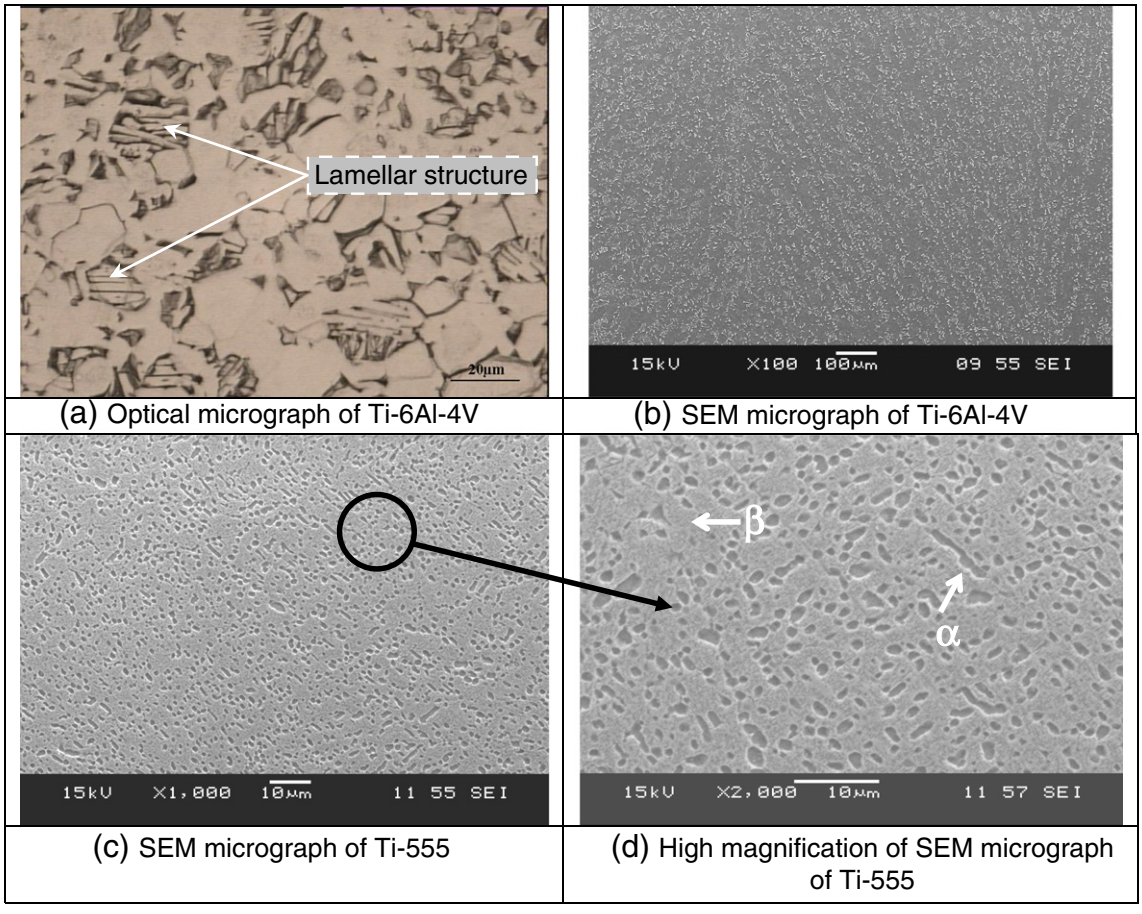


**Fig. 1.** Microstructure of the workpiece material used in this study before machining. (a) – α + β alloy Ti–6Al–4V. (c) – β alloy Ti-555.

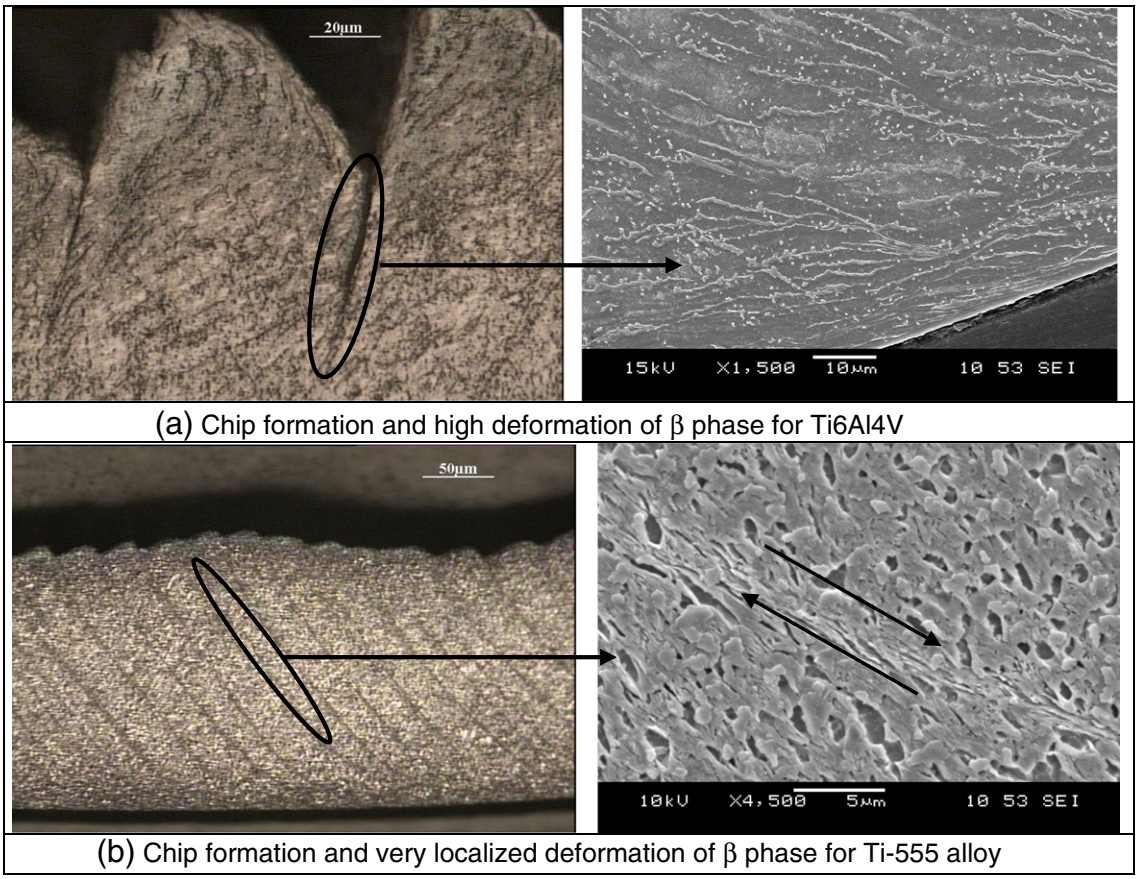


**Fig. 2.** Microstructure of the chip material obtained after machining. (a) – α + β alloy Ti–6Al–4V. (b) – β alloy Ti-555.

formation, friction coefficient, cutting temperature and tool wear. Tests were carried out on a heavy-duty lathe machine with an 11 kW motor drive, which generates a maximum torque of 1411 Nm. The spindle rotational speed ranges from 18 to 1800 rpm. Two alloys were chosen for machining experiments: (a) Ti–6Al–4V with duplex structure α / α + β, and average grain size around 10 µm (range from 5 µm–20 µm); (b) Ti-555 with average grain size around 1 µm (range from 0.5 µm–5 µm). Table 1 presents a summary of the chemical composition of both alloys. According to Fanning [10], Nouari et al. [20] and Bouchnak [9], the physical properties of the Ti–6Al–4V and Ti-555 alloys are summarized in Table 2.

Fig. 1(a), (b), (c) and (d) depicts the microstructure of each workpiece alloy before machining. The initial microstructure of the Ti–6Al–4V alloy, Fig. 1(a) and (b), consists of single phase α matrix. Inclusions of β grains can also be seen with average grain size of 10 µm (range of 5 µm–20 µm). Similarly, the initial microstructure of the β alloy Ti-555 is shown in Fig. 1(c) and (d). The microstructure consists of single phase β matrix with average size of α grains of 5 µm (range 1 µm–5 µm).

**Table 3**
Mechanical and thermal properties of the cutting tool substrate [5–7].

| Tool substrate | WC–6%Co |
|---|---|
| Hardness 25 °C ($HV_{10}$) | 1485 |
| Hot hardness 800 °C (kg/mm$^2$) | 600 |
| Density (g/cm$^3$) | 11.4 |
| Thermal conductivity (W/mK) | 45 |
| Thermal expansion ($10^{-6}$/K) | 6.1 |
| Modulus of elasticity (GPa) | 620 |
| Traverse rupture (GPa) | 2.2 |
| Poisson coefficient υ | 0.26 |

In this work, it has been found that the lamellar structure can be observed in α + β colonies (transformed β); particularly for the Ti–6Al–4V alloy. Fig. 1(a) shows the localization of the lamellar structure. This was previously confirmed by Benedetti and Fontanari [24].

Tests of Vickers hardness have been performed on different specimens under room temperature. The micro-hardness of the Ti–6Al–4V specimen was found to be about 317 $HV_{0.2}$ and that measured for the Ti-555 alloy to be about 379 $HV_{0.2}$. The Ti-555 is therefore 20% harder than Ti–6Al–4V. This result confirms the hard nature of the Ti-555 microstructure, which will have a direct impact on the machinability of this material, i.e. the level of cutting forces, tool wear, cutting temperature, etc.

Chips obtained after machining and presented in Fig. 2 were mounted with epoxy so that they stood on their edge in order to make the cross-section after polishing straight across its length. The polished chips and as-received workpiece material were etched with Kroll's reagent to reveal their microstructures. Micrographs of examined chips in Fig. 2 show clearly the deformation phenomenon inside the microstructure of both materials during the chip formation. However, the deformation process is different from one material to the other. It can be noted here that both chips given by machining Ti–6Al–4V and Ti-555 alloys were obtained with the same cutting conditions.

The examination of the deformed microstructure reveals very fine sizes of grains in the β alloy (Ti-555). In this material, the deformation process is localized in a very thin layer called primary shear zone while in the Ti–6Al–4V alloy the same process of deformation occurs in the whole microstructure, i.e. in α, β and α + β phases. Indeed, chips of the Ti–6Al–4V alloy have a very different microstructure compared to the initial Ti–6Al–4V alloy. For Ti-555 chips, apart from the primary shear zone, there is a very similar microstructure to that observed in the initial Ti-555 alloy.

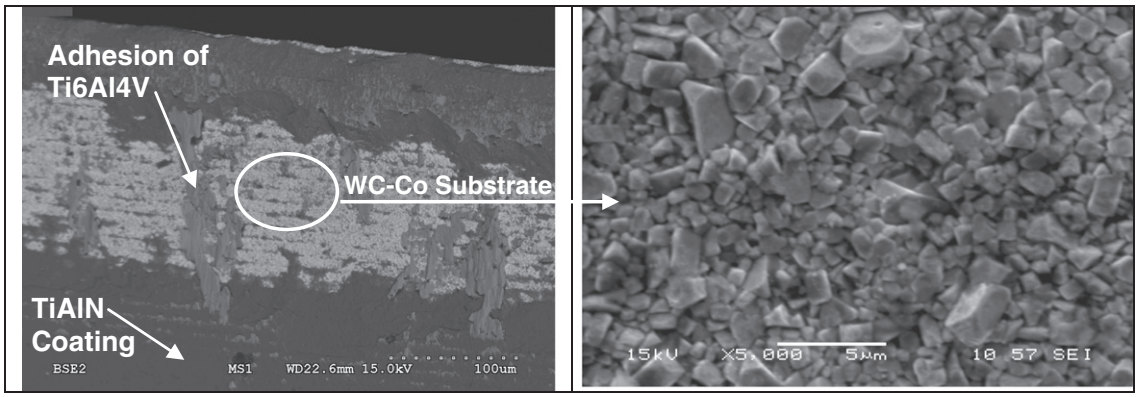


**Fig. 3.** SEM micrograph of cemented carbide tool (WC–6%Co).

To complete the analysis on the workpiece material, it is very important to know which temperature values are reached during machining. This gives us information on the β transus temperature and phase transitions in the two studied microstructures. A discussion of the cutting temperature parameter and its measurements has been more detailed in Section 2.4.

### 2.2. Cutting tool material

In this study, coated carbide inserts made of tungsten carbide (WC–Co) were used. All inserts had a single layer of TiAlN coating with average thickness of 4 µm.

This coating has a strong chemical stability, a low thermal conductivity and an anti-oxidation wear at 900 °C. TiAlN increases the surface hardness to approximately 3400–3600 HV, into improving the resistance to abrasive wear. The thermal conductivity of TiAlN coating is about 10 W/mK (at 20 °C).

Devillez et al. [27] state that TiAlN coating imparts an excellent crater resistance. Additionally, Singh et al. [28] and Castanho et al. [29] state that Al incorporated in TiAlN coating also can form superficial $Al_2O_3$ layer to improve the wear resistance and the chemical stability.

Table 3 presents a summary of the mechanical and thermal properties of cutting tools, whereas Fig. 3 depicts the microstructure of the cutting tool material.

Micrographs of Fig. 3 show that the inserts used consist of tungsten carbide WC with cobalt Co as binder. The chemical analysis on a polished surface inside the tool gives a composition with 6 wt.% of cobalt and no mixed carbides such as TiC, TaC or NbC have been detected. The Co binder is uniformly distributed and WC grains have sizes varying from 1 to 5 µm. In addition, it can be seen that the WC grain size is close to that of the Ti-555 grains.

### 2.3. Selection of the cutting parameters

Turning is a manufacturing process with a large number of interacting variables. The geometry produced in turning process is influenced by many variables, such as cutting speed, feed, depth of cut, etc. However, to facilitate the data collection, only four dominant factors were considered in the planning of experimentation. Cutting conditions (cutting speed and feed rate) and tool geometry (rake angle and flank angle) were considered as wear factors in this work to investigate the influence of microstructure on the cutting forces, friction coefficient, chip formation process, tool wear and cutting temperature. As shown by Table 4, experiments were carried out keeping cutting speed and rake angle at various levels. The range of each factor was selected based on the present day industrial requirements. The cutting length allowed by the machine capacity (about 1.5 m) provides a sufficient cutting time to reach the stationary regime of the cutting process (1.6 s for a cutting speed of 65 m/min).

All experiments were carried out with constant width of 3.5 mm. The other variables such as machine condition, variability in set up, etc. have been maintained constant throughout the experimentation. A three component Kistler® dynamometer was employed for cutting force measurements (Fig. 4). The forces reported are those for the process in a stable state with almost steady pulses.

Additional analyses have been performed using the friction coefficient. To understand physical phenomena during the chip formation, friction process have to be investigated at the tool–chip interface. The friction coefficient is an important parameter to characterize the nature of the tool–chip contact and tool wear depending on cutting conditions. According to the famous model of Merchant [13,14], the calculation of this parameter can be obtained using cutting forces measurements. In machining, the apparent friction coefficient (or average friction) is often defined as the ratio between the tangential force $F_t$ and the normal force $F_n$ [13,14].

$$\mu = \frac{F_t}{F_n} = \frac{F_a + F_c \tan\alpha}{F_c - F_a \tan\alpha} \quad (1)$$

where $\alpha$ is the rake angle, $F_c$: cutting force, $F_a$: feed force, $F_t$: friction force, $F_n$: normal force. For wear analysis, a toolmakers microscope (of 1 µm resolution) at 30× magnification was used. The wear

**Table 4**
Cutting conditions and tool geometry.

| | | | |
|---|---|---|---|
| Cutting speed $V_c$ (m/min) | 20 | 35 | 65 |
| Feed $f$ (mm/rev) | 0.1 | 0.1 | 0.1 |
| Rake angle (°) | 0 and 20° | 0 and 20° | 0 and 20° |
| Flank angle (°) | 7° | 7° | 7° |

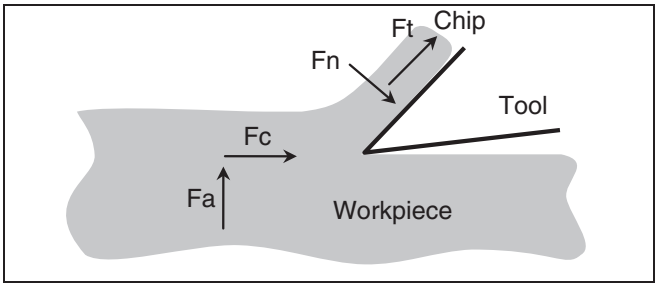


**Fig. 4.** Cutting forces and their direction in the machining plane. $F_c$: cutting force, $F_a$: feed force, $F_t$: tangential force, $F_n$: normal force.

**Table 5**
Mean temperature obtained by infrared camera technique (*Cedip camera*) when machining Ti-555 with WC–6%Co tool.

| Cutting speed (m/min) | Temperature (°C) |
|---|---|
| 20 | 628 |
| 65 | 761 |

surfaces were examined under a scanning electron microscope (SEM) equipped with energy X-ray spectrometer (EDS).

### 2.4. Temperature measurements

The cutting temperature was estimated using two techniques: the first technique is based on measurements with infrared camera (*Cedip camera*); and the second technique is based on an inverse measurement method using thermistor located behind the cutting tool edge. The last technique was previously developed by Battaglia et al. in Ref. [17].

(i) Infrared camera provides directly the thermal field which only gives an assessment of temperature levels. This technique allows a qualitative analysis, unfortunately, it cannot be used to determine with high precision temperature values on the cutting tool surface. This is due on one hand to the complexity of the instrumentation, and on the other hand to the confinement of the contact area between tool, chip and workpiece. Table 5 presents mean values of the cutting temperature in the case of machining Ti-555. These measurements were performed using two different cutting speeds ($V = 20$ m/min and $V = 65$ m/min).

(ii) In contrast with the first technique, the second method uses thermistors and provides an indirect measurement of the cutting temperature. The thermistor (very small thermocouple with diameter $d = 470$ μm) is placed in a hole made by electroerosion process inside the tool without embrittlement of its integrity. Thermistors are held fixed close to the cutting tool face. This makes possible to obtain measurements of the heat flux transmitted to the cutting tool. Using the inverse model, developed by Battaglia et al. in Ref. [17], an average temperature can be obtained with the measured heat flux taken as an input parameter of the model. We recall here that this type of measurement cannot be performed in the case of lubricated machining to avoid disturbance of the thermal field.

Table 6 shows the average temperatures estimated when machining Ti-555 with two cutting speeds ($V = 20$ m/min and $V = 65$ m/min).

As a conclusion on the temperature measurements study, it can be said that whatever the used cutting speed, no phase transition should be expected, since the corresponding cutting temperature remains less than the β transus of titanium alloys which is about 880 °C.

Therefore, no phase transition happens in the microstructure, confirming the assumption of Puerta Velasquez et al. in Ref. [18]. The later reported that only a severe shearing occurs in the titanium material during machining.

## 3. Results

### 3.1. Analysis of cutting forces

From the previously mentioned research, it has been found that the tool geometry (rake angle) and cutting conditions (cutting speed and feed) play an important role in the behavior of machined part. However, researchers have not paid much attention to study the effect of the microstructure on tool wear with varying cutting conditions and tool geometry simultaneously. Therefore, in the present work, an attempt has been made to examine the effect of various process parameters and tool geometry on the cutting forces, chip morphology, tool wear and temperature during machining two kinds of titanium microstructures: Ti–6Al–4V and Ti-555.

**Table 6**
Estimated temperatures during machining of Ti-555 using thermistors.

| Cutting speed (m/min) | Temperature (°C) |
|---|---|
| 20 | 450 |
| 65 | 800 |

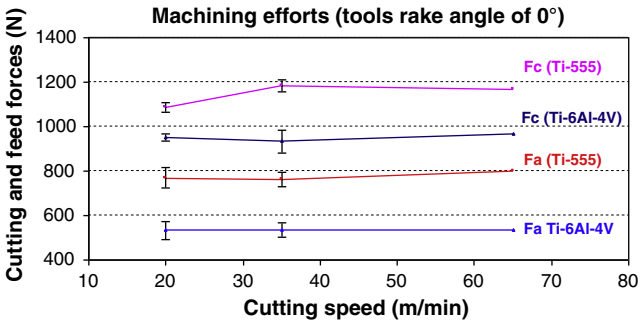


**Fig. 5.** Comparison between cutting forces obtained for Ti–6Al–4V and Ti-555 with a cutting tool rake angle of 0°.

Measurement of cutting forces in turning is essential for assessing the performance of the machining process. Cutting forces therefore provide a basis for process planning, machine tool design and cutter geometry optimization to minimize production cost and time. Therefore, the measurement of the cutting force is an important parameter in machining processes to achieve high accuracy and productivity. In addition to the friction in the tool/chip interface, cutting forces depend on two main factors: area of the primary and secondary shear planes, and shear strength of the work material at these planes [15,16].

Figs. 5 and 6 illustrate cutting forces ($F_c$) and feed forces ($F_a$) generated during machining. The evolution of machining efforts is plotted as a function of the cutting speed $V_c$.

It can be observed from Figs. 5 and 6 that $F_c$ is the dominant force component. Therefore, the discussion on cutting forces is focused on the cutting force due the weak variation of feed forces. As seen in Fig. 6, the feed force remains stable for all conditions.

First of all, it can be noted in Fig. 5, a stabilization of cutting forces with high cutting speeds (35 m/min and 65 m/min). However, a slight increase is still noticeable on the cutting force of the Ti-555 alloy when cutting speed increases from 20 m/min to 65 m/min. During machining the Ti–6Al–4V alloy with a tool rake angle of 20° (Fig. 6), a reduction of cutting forces is noticed when the cutting speed increases. This is quite normal considering the thermal softening of the material due to the temperature rise during machining. In other words, when the cutting speed increases, the temperature increases too and this is followed by a decrease in the yield stress level of the alloy. The material deforms under these conditions

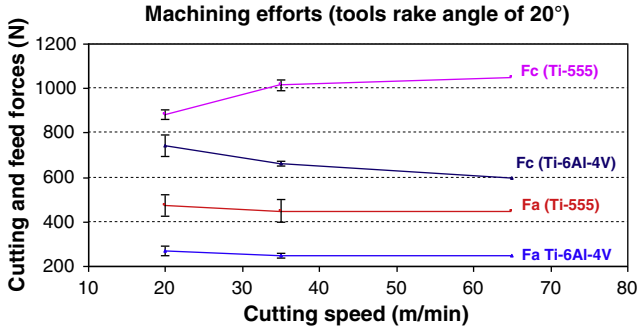


**Fig. 6.** Comparison between cutting forces obtained for Ti–6Al–4V and for Ti-555 with a cutting tool rake angle of 20°.

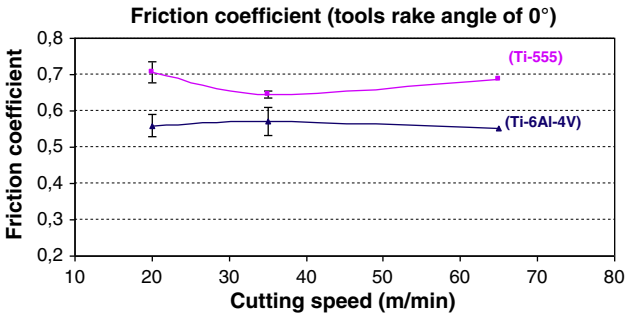


**Fig. 7.** Evolution of the friction coefficient of tools with 0° rake angle.

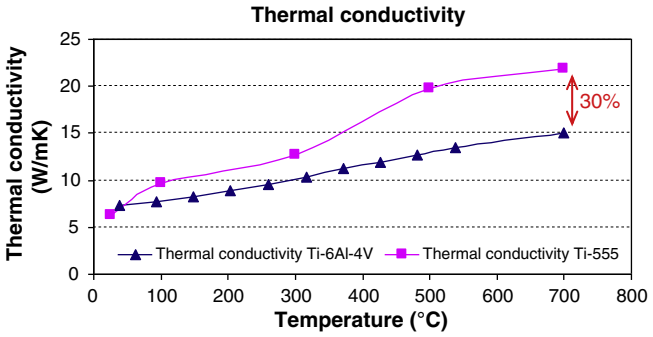


**Fig. 9.** Evolution of thermal conductivities of Ti-555 and Ti–6Al–4V with cutting temperature.

much more easily and without significant effort. This trend is expected because machining becomes more adiabatic and the heat generated in the shear zone cannot be conducted away during the very short interval of time during which the material passes through this zone. Therefore, the temperature rise softens the material aiding grain boundary dislocation and thus reducing cutting forces as seen from Fig. 6.

However, the cutting speed cannot be increased significantly pretext to further reduce the effort because of the significant increase (simultaneously) of the tool wear. On the other hand, an increase in the cutting force level of Ti-555 with 20° tool rake angle can be observed when increasing the cutting speed. This tendency can be explained by the high strain rate sensitivity of the Ti-555 alloy.

According to Fig. 5, the comparison between generated cutting forces shows a clear difference between Ti–6Al–4V and Ti-555. This difference is ranged from 12.3% to 21.1% for the cutting force and from 30.1% to 33.4% for the feed force. This result confirms the poor machinability (previously announced) of the Ti-555 alloy compared to that of the Ti–6Al–4V under the same machining conditions. The trend given by tools with a rake angle of 0° is confirmed by tools with a rake angle of 20°. The difference may reach 42.9% for some cutting conditions ($V = 65$ m/min and $\alpha = 20°$) (see Fig. 6).

In addition, it was found from Figs. 5 and 6 that the cutting force obtained with the rake angle of 20° was weak compared to that of machining with 0° rake angle at all levels of considered parameters. This has been attributed to the fact that high values of the rake angle may reduce the friction along the cutting edge between tool and workpiece; see the evolution of the fiction coefficient in the next subsection (Section 3.2).

### 3.2. Friction evolution

Figs. 7 and 8 show the variation of friction coefficient values at various cutting conditions. In all tests, this parameter is more important with tools of 0° geometry compared to those with 20° rake angle. This is due to the reduction of the cutting temperature and contact length. This reduction is often followed by a reduction in frictional forces at the tool–workpiece interface. Low cutting temperatures reduce adhesion tendency of the cutting tool and promote contact area restriction. Reduction of the tool–chip contact length is expected to occur, as well as promotion of the plastic flow at the backside of the chip and overall reduction of temperature.

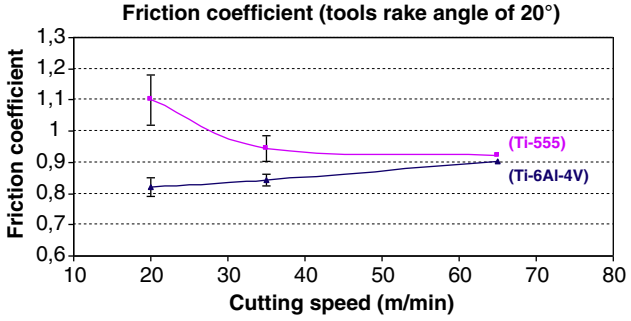


**Fig. 8.** Evolution of the friction coefficient of tools with 20° rake angle.

The results presented above (in Figs. 7 and 8) show a higher friction coefficient for Ti-555 compared to Ti–6Al–4V. Thus, the following assumptions can be presented: the contact area at the tool–chip interface can be considered as a sticking contact-type for Ti-555 in the case of machining with tools of 0° rake angle. Therefore, a connection can be made between the nature of the contact (sticking) and the tendency of Ti-555 to adhere to the cutting face of the tool. In contrast, the tool–chip contact can be of a sliding type in the case of Ti–6Al–4V because of the low values of friction (see Fig. 7). In the case of machining with tools of 20° rake angle (Fig. 8), the reduction in friction coefficient for the Ti-555 indicates contact of sliding type more than sticking one. Contrary to this trend, increasing friction for the Ti–6Al–4V alloy indicate sticking contact.

### 3.3. Tool wear

This subsection focuses on the analysis of tool failure modes and wear mechanisms when machining considered titanium alloys. Before starting the analysis, it very important to be reminded of the evolution of thermal conductivities for these two materials with temperature (Fig. 9). This has a direct impact on the evolution of tool wear. The data used for plotting Fig. 9, were obtained by measuring thermal conductivities using “Hot Disk” method for several specimens under different temperatures [23]. The high temperatures were close to those obtained during machining the same materials.

Ti-555 and Ti–6Al–4V alloys show a clear difference of about 30% in their thermal conductivities at 700 °C (Fig. 9). At high temperatures, the Ti-555 alloy conducts heat better than the Ti–6Al–4V alloy. This result is very interesting since it allows us to explain the morphology observed of formed chips and the variation in cutting forces. Indeed, a low thermal conductivity promotes chip segmentation and thus a reduction of the machining efforts; this is the case for Ti–6Al–4V alloy [19]. When the thermal conductivity increases, the heat stored in the machined material is discharged to the chip and then the ability of the machined material to soften is reduced. Under these conditions, the machining efforts will not fall because of the material flow stress which remains high even at very high temperatures, as in the case for the Ti-555 alloy. Based on these findings, the degradation modes of the cutting tool could be of a mechanical type for Ti-555 (abrasion mode) and physico-chemical for Ti–6Al–4V (adhesion and diffusion modes).

It has been observed from the SEM analysis in Figs. 10 and 11 that the cutting tool encounters severe thermal and mechanical loading when machining titanium alloys. This can be supported by the level

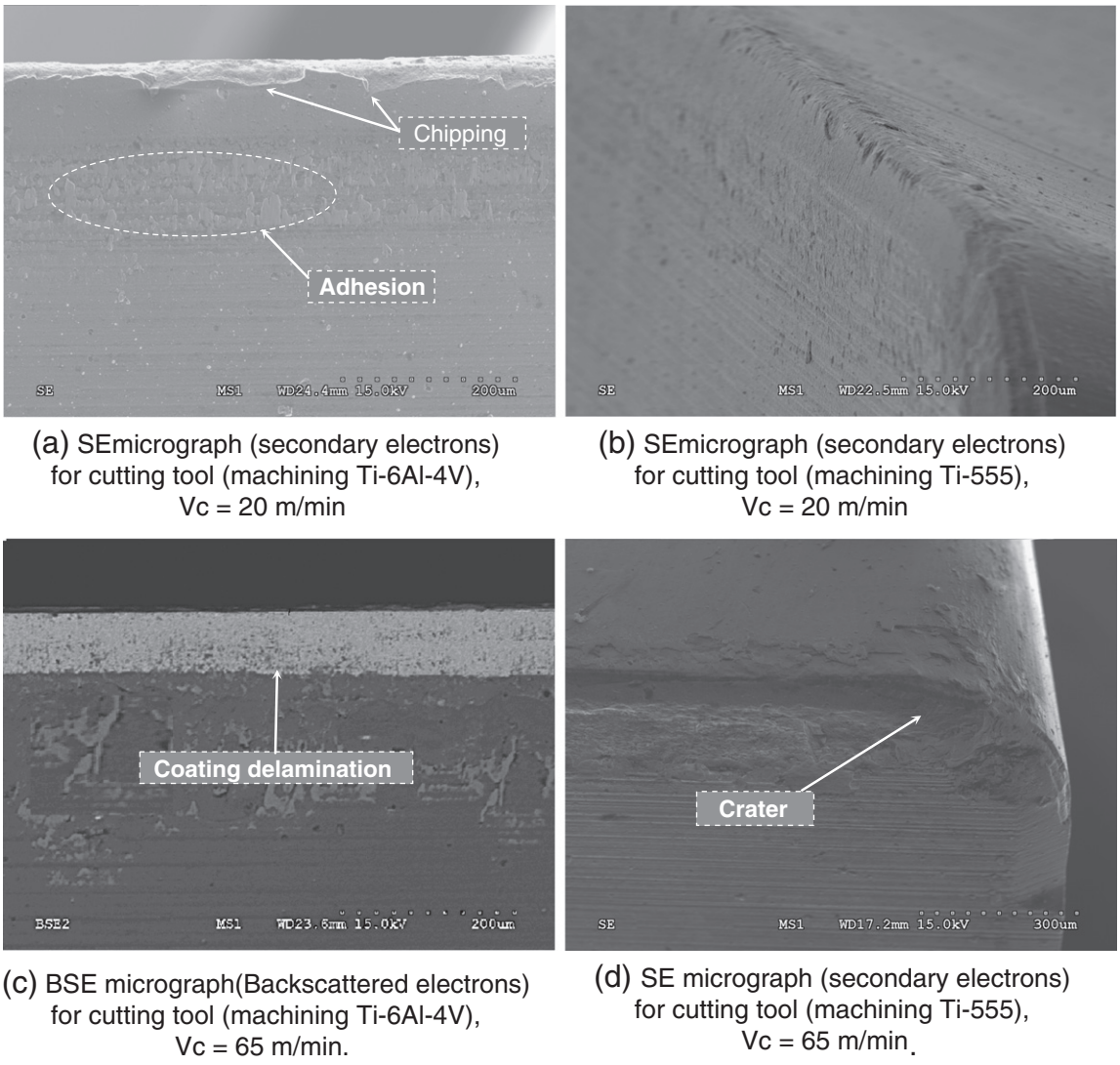


(a) SEmicrograph (secondary electrons) for cutting tool (machining Ti-6Al-4V), Vc = 20 m/min

(b) SEmicrograph (secondary electrons) for cutting tool (machining Ti-555), Vc = 20 m/min

(c) BSE micrograph(Backscattered electrons) for cutting tool (machining Ti-6Al-4V), Vc = 65 m/min.

(d) SE micrograph (secondary electrons) for cutting tool (machining Ti-555), Vc = 65 m/min.

**Fig. 10.** SEM images (BSE and SE micrographs) of the tool wear when machining Ti–6Al–4V and Ti-555 alloys with different cutting speeds (rake angle 0°).

of the measured cutting temperature (about 750–800 °C for $V =$ 65 m/min) and high recorded cutting forces (about 1000 N). In addition, other works previously showed that the cutting pressure can also attain large values (about 1–1.5 GPa) [25,26].

The high stresses and high temperatures generated close to the cutting edge have great influence on the tool wear rate and on tool life. As the cutting speed and feed increase, the cutting temperature and stress prevailing over the cutting edge increase too.

In the case of tools with 0° rake angle, the extent of the area affected by the wear is greater for Ti-555 than for Ti–6Al–4V. At 20 m/min for example, it is about 120 μm for the Ti–6Al–4V while about 160 μm for Ti-555 (Fig. 10(a) and (b)). This is mainly due to the fact that the increase in cutting forces for the Ti-555 generates higher stress on the cutting edge. The hardness of the material also contributes to the heavy wear edge. Micrographs also show delamination of the coating layer on the tool surface during machining Ti–6Al–4V at 65 m/min. This is not the case for the Ti-555 alloy under the same cutting speed (Fig. 10(c) and (d)).

The delamination phenomenon is difficult to analyze because it can have both thermal and mechanical origins. This is partly due to the complex interaction between various physical factors that control delamination: intrinsic properties of the coating, tool and those of the interaction between the substrate, coating and workpiece. However, it is possible to attribute the origin of delamination to chemical reactions. During cutting of Ti–6Al–4V, adhesion occurring at the tool–chip interface is the main harbinger of the delamination problem.

At low cutting speeds, adhesive wear mode was observed during machining titanium alloys (Fig. 10). The location of the adhesion wear is greater in the case of Ti–6Al–4V compared to Ti-555. For Ti-555, the wear results show that the predominant degradation process is abrasion wear (Fig. 10(b)).

As shown by the EDS analysis illustrated in Fig. 12, particle debris are deposited on the tool surface during machining Ti–6Al–4V as successive layers when chips scroll to the surface. This leads to the adhesive wear mode. The latter is highlighted by the change in the tool geometry and debonding of the coating (Fig. 11(c)).

Auger Electron Spectroscopy (AES) Surface Analysis was also used to verify the occurrence of diffusion process. This technique shows the evolution of the chemical composition at the interface between two different materials. Diffusion profiles were obtained along two lines located in the adhesion zone and inside the worn tool. The AES Surface Analysis performed on the cutting tool (Fig. 13(a)) show along L1 and L2 in Fig. 13(b) and (c) respectively the evolution of chemical species from the interface between the adhered material on the tool surface till some micrometers inside the tool substrate. It is clearly shown from this figure that diffusion process occurred between the machined titanium alloys and cutting tool during

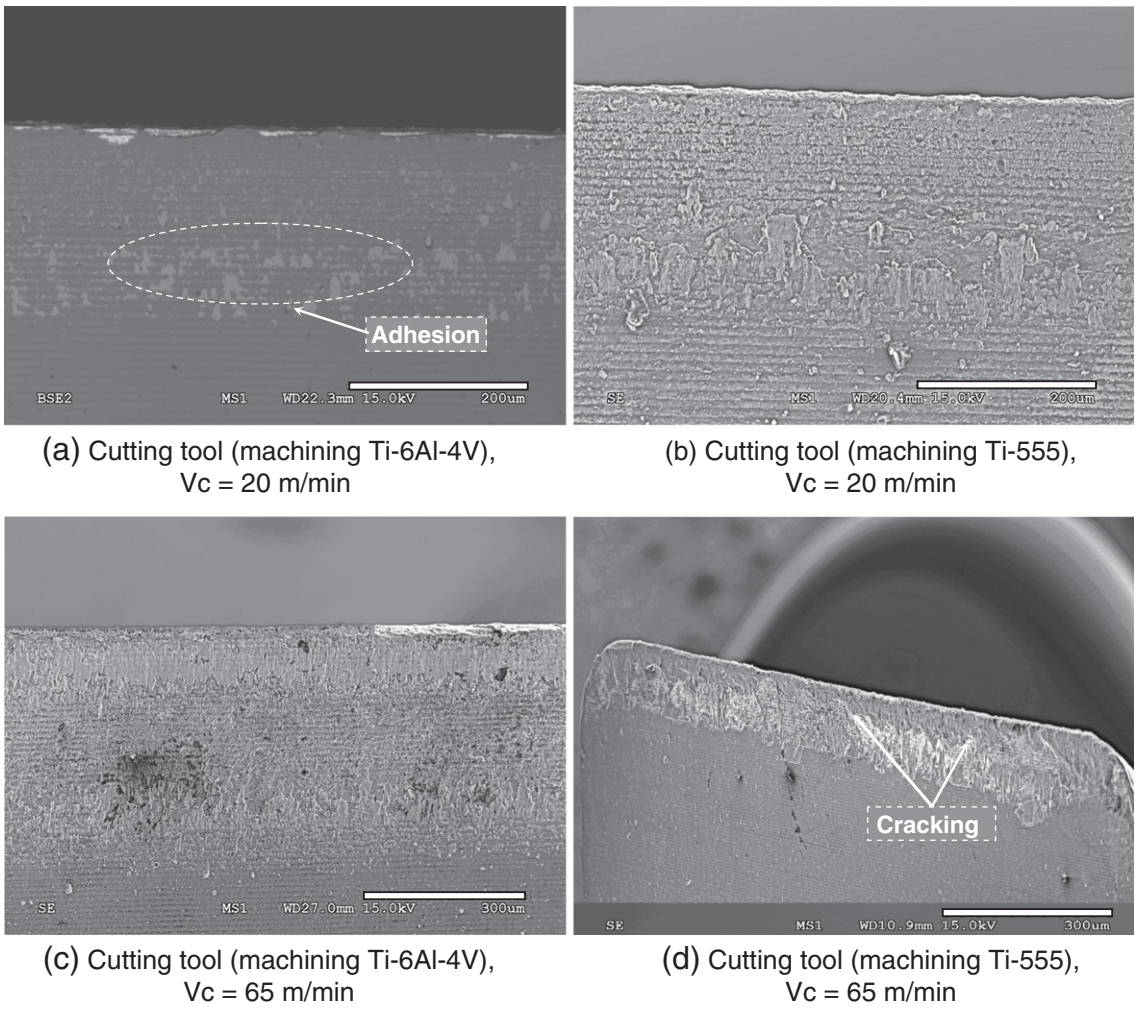


**Fig. 11.** SEM images of the tool wear when machining Ti–6Al–4V and Ti-555 alloys (rake angle 20°).

machining. Diffusion profiles clearly show the diffusion of chemical species from the machined material (Ti, Al, and V) to the cutting tool (W, Co, and C) and vice versa. This diffusion process can be considered as a process which can generate adhesion wear of the cutting tool and/or delamination of coating.

During machining Ti-555 at 65 m/min, a process of cracking starts resulting in a collapse of the cutting edge (Figs. 10(d) and 11(d)). This is produced by the combined effect of high pressures and large strain rates in the tool (substrate and coating).

Adhesive wear layers on the tool surface were measured using a profilometer in the case of machining Ti–6Al–4V. Fig. 14 shows the evolution of the adhesive layer extent vs. cutting speed.

It appears from this result that the adhesive wear increases with the cutting speed and it stabilized at high speeds. This may due to

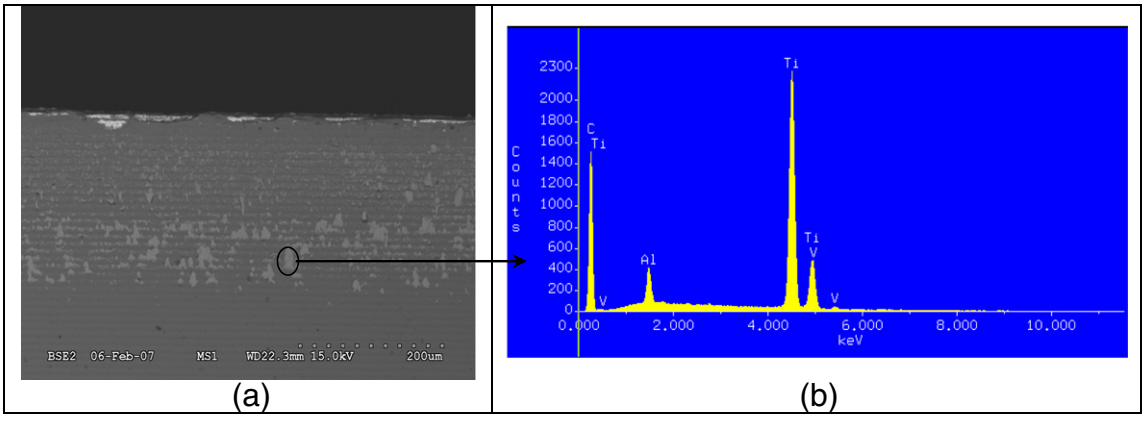


**Fig. 12.** EDS measurements of the adhered material (Ti–6Al–4V) on the rake face. $V = 20$ m/min, rake angle 0°.

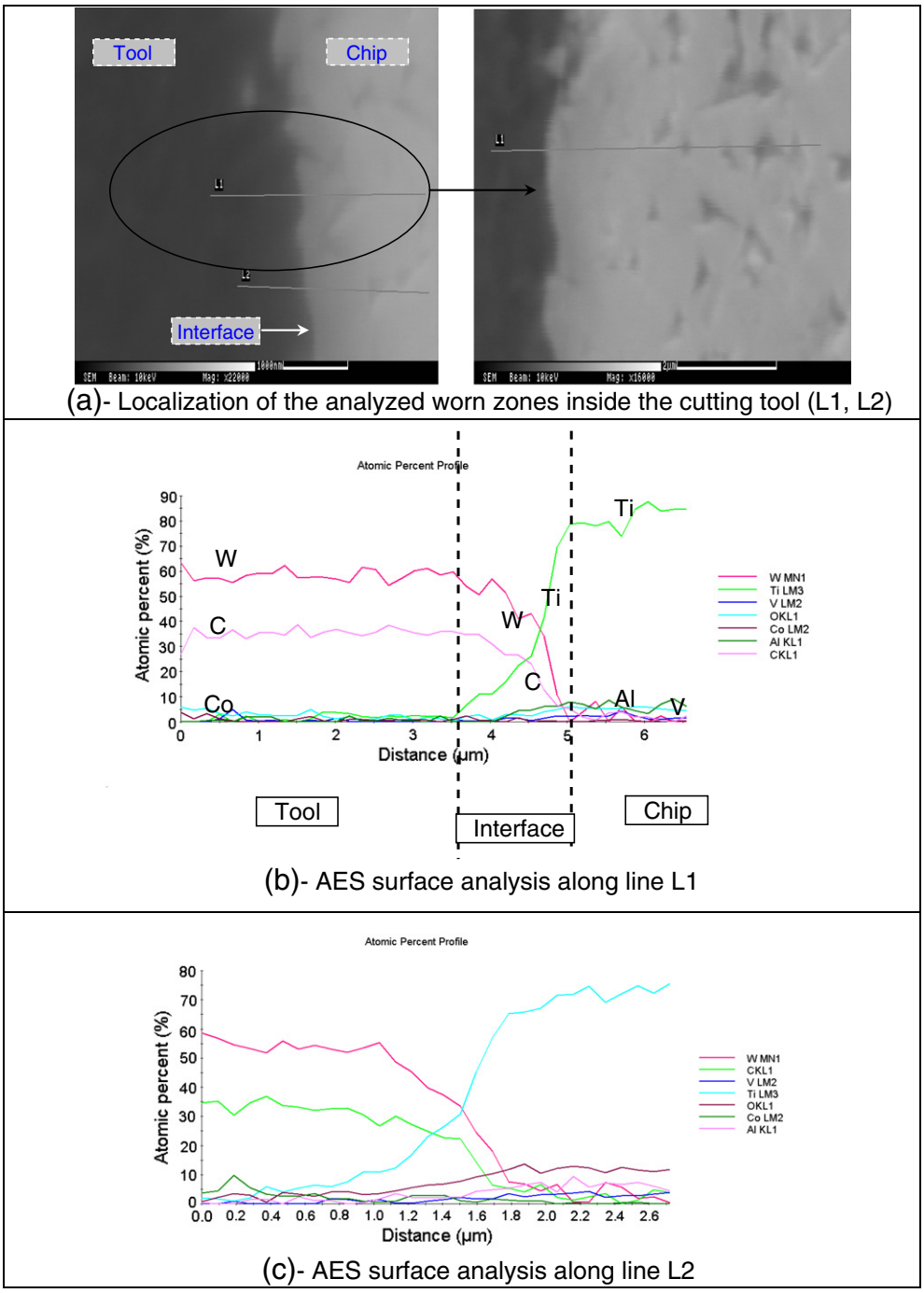


**Fig. 13.** Diffusion profiles obtained at the tool–chip interface by AES surface analysis along Lines L1 and L2 in the tool–chip interface and inside the cutting tool. Cutting conditions are identical to those of Fig. 12.

the diffusion process between titanium alloy and the cutting tool at the interface.

In some cases and under the combined effect of pressure and temperature, welds are formed between tool and chip. With permanent mechanical stress (during machining), these welds are broken thereby causing chipping of the cutting surface. The irregularity on the tool surface can constitute attachment points for chip debris. By accumulating, they eventually form a detrimental macroscopic deposit on the cutting edge. This phenomenon has been observed for cutting tools when machining the Ti–6Al–4V alloy under low cutting speeds (see Figs. 10(a) and 11(a)).

Topographical survey using the profilometer (Fig. 15) confirmed that the tool wear exhibited when the machining of the Ti-555 alloy changes the geometry of the cutting edge. Cracking is due to a fatigue phenomenon of the cutting edge followed by a break of the tool under cyclic loading during machining. The tool with 20° rake angle showed resistance to wear by fatigue and plastic deformation in the case of Ti-555. Indeed, this geometry improves the flow of chips and material deformation.

In the case of Ti–6Al–4V, the average grain size is about 10 µm and the measured micro-hardness is in the range of 317 $HV_{0.2}$. For the Ti-555, the microstructure is homogeneous and the grain size is

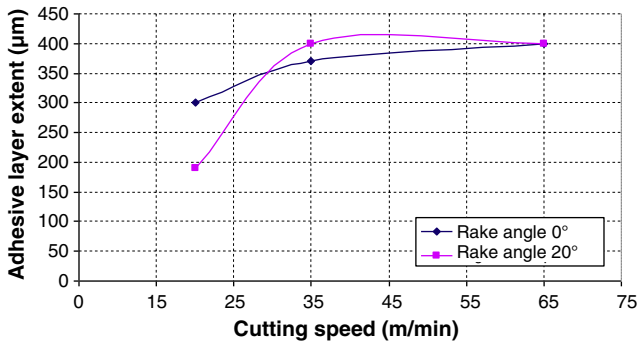


**Fig. 14.** Evolution of the adhesive layer extent on the tool surface during machining Ti–6Al–4V with different cutting speeds.

about 1 µm with a microhardness of 379 $HV_{0.2}$. From a metallurgical point of view, the major difference between the Ti–6Al–4V and Ti-555 is due to fineness of the microstructure. This generally leads to a higher mechanical strength. However, this will strongly influence the machinability of the machined materiel and then tool wear as confirmed by Powell and Duggan [21] and by Arrazola et al. in Ref. [22]. In addition, the Ti-555 is an alloy of β-type (near-β titanium alloy), with the presence of betagenic elements, such as chromium, for example, which limits the ability of the material to deform during machining.

Based on the results from the experimental tests, we can give some ideas to improve the machining of the two alloys studied in this article. It is possible to increase the cutting speed in the case of machining Ti–6Al–4V, which causes the increase in temperature at the interface tool/material and therefore a significant softening of the machined material. Consequently, cutting efforts will be lower. This solution cannot be applied in the case of Ti-555 because of its high strain rate sensitivity.

On the other hand, the improvement of the machining of Ti–6Al–4V can be carried out by changing the geometry of the tool. Increasing rake angle facilitates chip flow; this will cause reduction in cutting efforts and pressure. This improvement can also be applied to the machining of Ti-555.

## 4. Conclusion

In this study, several analyses (SEM, EDS, AES, infrared camera and profilometer analysis) confirmed that the differences in machinability and microstructure of tested titanium alloys have an important impact on tool wear. The low machinability of titanium alloys due to the low thermal conductivity and high microhardness of these materials leads to severe and premature tool wear in dry machining process.

Thermal and mechanical analyses revealed two important phenomena. First, the thermal softening which results in a lowering of the yield stress when the temperature increases, and secondly the strain rate hardening which increases the hardness of the material. Increasing the hardness in machining implies systematically an increase in the level cutting force. Indeed, an increase in the cutting speed raises the temperature at the tool–workpiece interface, and increases at the same time the strain rate. Both phenomena occur simultaneously and reflect two opposite effects. It was concluded from different analyses that the Ti–6Al–4V alloy is more sensitive to thermal softening while the Ti-555 alloy undergoes a strain rate hardening which results in a higher yield stress. Consequently, the difference in cutting forces between the two alloys was found to be about 20%.

Microstructure analysis shows two distinct structures. A coarse structure for the Ti–6Al–4V alloy with a mean grain size around 10 µm and with α phase as more ductile matrix of the alloy. Ti-555 has a nodular structure with very fine grains of about 1 µm with a much harder β phase. These differences mean that the Ti-555 (about 20% harder than the usual Ti–6Al–4V alloy) is more difficult to cut. The very fine microstructure and the presence of chromium (Cr) may promote strain hardening behavior of this alloy.

No phase transformation was observed for both titanium materials. For the Ti-555, β grains experiences high plastic deformation and increases the microhardness of the workpiece inducing then abrasion wear process for the cemented carbide tools. For the Ti–6Al–4V microstructure, the temperature rise induces a thermal softening process in the workpiece and generates adhesive and diffusion wear modes for cutting tools.

## References

[1] Boyer RR. An overview on the use of titanium in the aerospace industry. Mater Sci Eng 1996;213A:103–14.
[2] Ginting A, Nouari M. Surface integrity of dry machined titanium alloys. Int J Mach Tools Manuf 2009;49(3–4):325–32.
[3] Clément N, Lenain A, Jacques PJ. Mechanical property optimization via microstructural control of new metastable beta titanium alloys, processing and characterizing titanium alloys overview. JOM 2007:50–3.
[4] Clement N, et al. In: Howe JM, et al, editor. Proc. Int. Conf. Solid — Solid Phase Transformations in Inorganic Materials 2005. Warrendale, PA: TMS; 2005. p. 603–8.
[5] Nouari M, Ginting A. Wear characteristics and performance of multi-layer CVD-coated alloyed carbide tool in dry end milling of titanium alloy. Surf Coat Technol 2006;200(18–19):5663–76.
[6] Ginting A, Nouari M. Experimental and numerical studies on the performance of alloyed carbide tool in dry milling of aerospace material. Int J Mach Tools Manuf 2006;46(7–8):758–68.
[7] Ginting A, Nouari M. Optimal cutting conditions when dry end milling the aeroengine material Ti-6242S. J Mater Process Technol 2007;184:319–24.
[8] Komanduri R, Turkovich BFV. New observations on the mechanism of chip formation when machining titanium alloys. Wear 1981;69:179–88.
[9] Bouchnak TB. Etude du comportement en sollicitations extrêmes et de l'usinabilité d'un nouvel alliage de titane aéronautique. PhD thesis, ref. 2010-ENAM-0051, Arts et Métiers ParisTech - Centre d'Angers; 2010.

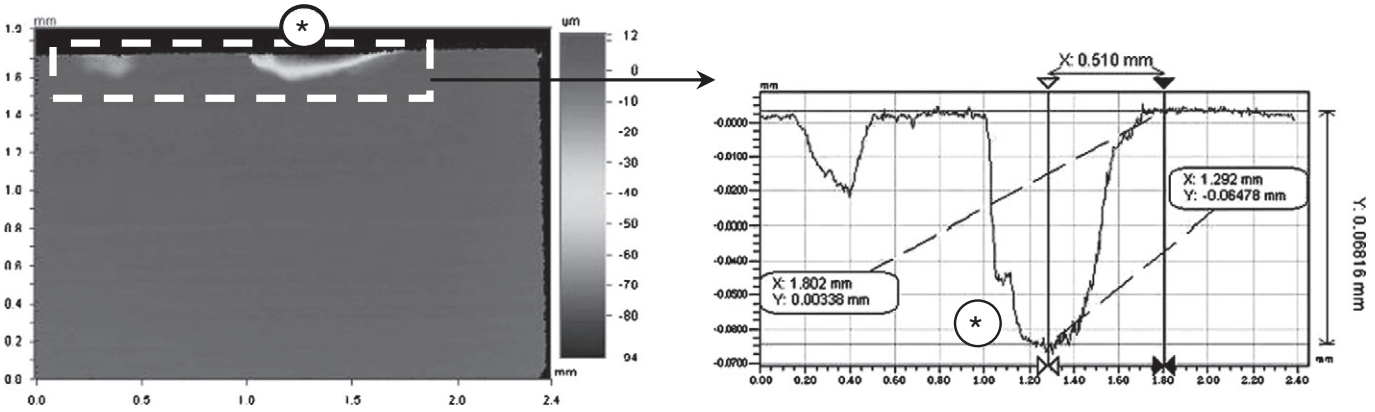


**Fig. 15.** Worn tool when machining Ti-555 analyzed by optical profilometer. * Notched wear with depth of 61 µm.

[10] Fanning JC. Properties of TIMETAL 555 (Ti–5Al–5Mo–5V–3Cr–0.6Fe). JMEPEG 2005;14:788–91.
[11] Nyakana SL, Fanning JC, Boyer RR. JMEPEG 2005;14:799–811.
[12] Semiatin SL, Seetharaman V, Ghosh AK. Plastic flow, microstructure evolution, and defect formation during primary hot working of titanium and titanium aluminide alloys with lamellar colony microstructures. Philos Trans R Soc A: Math, Phys Eng Sci 1999;357(1756):1487–512.
[13] Jackson M, Dashwood R, Christodoulou L, Flower H. The microstructural evolution of near beta alloy Ti–10V–2Fe–3Al during subtransus forging. Metall Mater Trans A Phys Metall Mater Sci 2005;36:1317–27.
[14] Merchant E. Mechanics of the metal cutting process I. Orthogonal cutting and a type 2 chip. J Appl Phys 1945;16:267–75.
[15] Merchant E. Mechanics of the metal cutting process II. Plasticity conditions in orthogonal cutting. J Appl Phys 1945;16:318–24.
[16] Diniz Anselmo Eduardo, Micaroni Ricardo. Cutting conditions for finish turning process aiming: the use of dry cutting. Int J Adv Manuf Technol 2002;42:899–904.
[17] Battagliaa JL, Coisb O, Puigsegura L, Oustaloupb A. Solving an inverse heat conduction problem using a non-integer identified model. Int J Heat Mass Transfer 2001;44: 2671–80.
[18] Puerta Velasquez JD, Bolle B, Chevrier P, Geandier G, Tidu A. Metallurgical study on chips obtained by high speed machining of a Ti–6 wt.%Al–4 wt.%V alloy. Mater Sci Eng A 2007;452–453:469–74.
[19] Abdel-Aal HA, Nouari M, EL Mansori M. Tribo-energetic correlation of tool thermal properties to wear of WC–Co inserts in high speed dry machining of aeronautical grade titanium alloys. Wear 2009;266:432–43.
[20] Nouari M, Calamaz M, Girot F. Mécanismes d'usure des outils coupants en usinage à sec de l'alliage de titane aéronautique Ti–6Al–4V. CR Mécanique 2008;336: 772–81.
[21] Powell BE, Duggan TV. Predicting the onset of high cycle fatigue damage: an engineering application for long crack fatigue threshold data. Int J Fatigue 1986;8: 187–94.
[22] Arrazola P-J, Garay A, Iriarte L-M, Armendia M, Marya S, Le Maître F. Machinability of titanium alloys (Ti6Al4V and Ti555.3). J Mater Process Technol 2009;209:2223–30.
[23] He Yi. Rapid thermal conductivity measurement with a hot disk sensor: part 1. Theoretical considerations. Thermochim Acta 2005;436:122–9.
[24] Benedetti M, Fontanari V. The effect of bi-modal and lamellar microstructures of Ti–6Al–4V on the behaviour of fatigue cracks emanating from edge-notches. Fatigue Fract Eng Mater Struct 2004;27:1073–89.
[25] Ezugwu EO, Wang ZM. Titanium alloys and their machinability — a review. J Mater Process Technol 1997;68:262–74.
[26] Komanduri R. Some clarifications on the mechanics of chip formation when machining titanium alloys. Wear 1982;76:15–34.
[27] Devillez A, Schneider F, Dominiak S, Dudzinski D, Larrouquere D. Cutting forces and wear in dry machining of Inconel 718 with coated carbide tools. Wear 2007;262(7–8):931–42.
[28] Singh Gill S, Singh R, Singh H, Singh J. Investigation on wear behaviour of cryogenically treated TiAlN coated tungsten carbide inserts in turning. Int J Mach Tools Manuf 2011;51(1):25–33.
[29] Castanho J, Vieira M. Effect of ductile layers in mechanical behaviour of TiAlN thin coatings. J Mater Process Technol 2003;143:352–7.